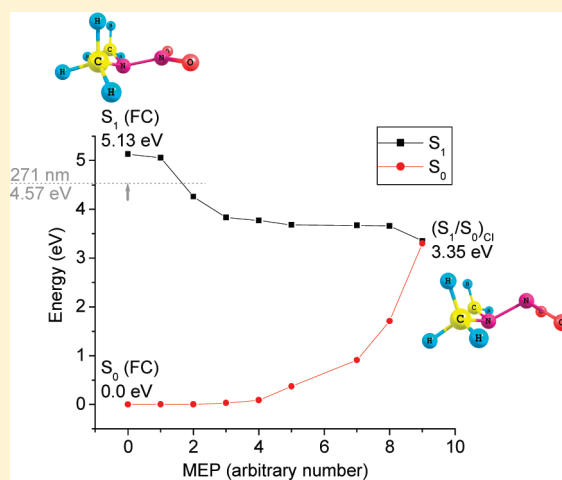


Ultrafast S_1 to S_0 Internal Conversion Dynamics for Dimethylnitramine through a Conical IntersectionYuanqing Guo, Atanu Bhattacharya,[†] and Elliot R. Bernstein*

Department of Chemistry, Colorado State University, Fort Collins, Colorado 80523-1872, United States

ABSTRACT: Electronically nonadiabatic processes such as ultrafast internal conversion (IC) from an upper electronic state (S_1) to the ground electronic state (S_0) through a conical intersection (CI), can play an essential role in the initial steps of the decomposition of energetic materials. Such nonradiative processes following electronic excitation can quench emission and store the excitation energy in the vibrational degrees of freedom of the ground electronic state. This excess vibrational energy in the ground electronic state can dissociate most of the chemical bonds of the molecule and can generate stable, small molecule products. The present study determines ultrafast IC dynamics of a model nitramine energetic material, dimethylnitramine (DMNA). Femtosecond (fs) pump–probe spectroscopy, for which a pump pulse at 271 nm and a probe pulse at 405.6 nm are used, is employed to elucidate the IC dynamics of this molecule from its S_1 excited state. A very short lifetime of the S_1 excited state ($\sim 50 \pm 16$ fs) is determined for DMNA. Complete active space self-consistent field (CASSCF) calculations show that an $(S_1/S_0)_{CI}$ CI is responsible for this ultrafast decay from S_1 to S_0 . This decay occurs through a reaction coordinate involving an out-of-plane bending mode of the DMNA NO_2 moiety. The 271 nm excitation of DMNA is not sufficient to dissociate the molecule on the S_1 potential energy surface (PES) through an adiabatic NO_2 elimination pathway.



INTRODUCTION

Decomposition of energetic materials (e.g., explosives, propellants, pyrotechniques, fuels) can be initiated by different processes, including sparks, arcs, shocks, compression waves, and light. These events induce electronic excitation in energetic molecules.^{1–14} In principle, a number of photochemical and photophysical processes can occur following electronic excitation of an energetic molecule: these include radiative transitions, such as fluorescence and phosphorescence, nonradiative transitions, such as internal conversion (IC) and intersystem crossing (ISC), and excited state photochemistry. IC is particularly important for the initial steps of the decomposition of energetic molecules because, by utilizing this process, energetic molecules can transfer electronic energy to the vibrational degrees of freedom of the ground electronic state potential energy surface (PES).¹⁵ This vibrational energy can eventually dissociate the covalent bonds of an energetic molecule and begin the chain reaction to release the stored chemical energy of energetic materials. Additionally, ultrafast IC is often found to occur through one or more conical intersections (CIs, minimum energy crossing points) of adiabatic PESs, thereby generating an ultra short (fs) lifetime for the excited electronic state S_1 . Such ultra short lifetimes for excited electronic states can also play an important role in the energy material sensitivity to initiation events.¹⁵ CIs have been firmly established to be key features in the excited electronic state chemistry of polyatomic molecules.^{16–18} The

concept of a CI was first introduced by von Neumann and Wigner¹⁹ and has been now recognized as essential for describing the ultrafast dynamics and mechanisms for deactivation of polyatomic molecules from their excited electronic states to their ground electronic surfaces.^{20–24}

Manaa et al.²⁵ explored the electronic properties of a single $\text{N}-\text{NO}_2$ moiety in order to explain the behavior of nitramine energetic materials. They consider the role of singlet–triplet ISC through ab initio quantum chemistry calculations, in order to model the pathway for fast nonradiative relaxation. They predicted a singlet–triplet minimum energy crossing point $(T_1/S_0)_{CI}$ to establish a nonradiative transition mechanism to deactivate the T_1 state of a nitramine. They further proposed that existence of such a $(T_1/S_0)_{CI}$ can generate fast nonradiative energy transfer from T_1 to S_0 , but they did not consider the role of the S_1 excited state IC through a singlet–singlet minimum energy crossing point $(S_1/S_0)_{CI}$ for vibrational excitation of the nitramine S_0 state.

In the present study, the fast IC from S_1 to S_0 of dimethylnitramine (DMNA), a model energetic material, is determined, and the role played in this process by the CI of S_1 and S_0 adiabatic

Special Issue: A: David W. Pratt Festschrift

Received: September 24, 2010

Revised: January 14, 2011

Published: February 25, 2011

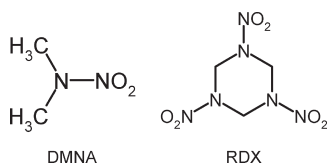


Figure 1. Chemical structures of the nitramine energetic material RDX and model system DMNA.

PESs ($(S_1/S_0)_{CI}$ CI) is addressed and evaluated. DMNA is considered to be a simple analogue molecule of a nitramine energetic material, such as RDX (see Figure 1 for the structure of DMNA and RDX). DMNA has only one nitramine (N–NO₂) moiety, whereas RDX has three (see Figure 1). Determination of the S_1 excited electronic state lifetime of DMNA and exploration of its nonadiabatic relaxation pathways involved in the fast IC from S_1 to S_0 can provide many details of the electronic properties of, and processes available to, a single nitramine energetic moiety.

The decomposition of DMNA from excited electronic states has been recently investigated in our laboratory.^{15b} Experimentally, we determined that DMNA decomposes through a nitro-nitrite isomerization mechanism at 226 nm excitation, and generates an NO molecule as an initial product. Theoretical calculations show that the DMNA molecule is excited to the S_2 electronic state following 226 nm excitation, and the $(S_2/S_1)_{CI}$ CI between the S_2 and S_1 electronic states along the nitro-nitrite isomerization reaction coordinate plays an important role in the overall decomposition of DMNA.

The present report discusses the existence of an $(S_1/S_0)_{CI}$ CI between adiabatic S_1 and S_0 PESs and determines the ultrafast relaxation IC of DMNA from S_1 to S_0 electronic states. The IC dynamics are determined experimentally by pump–probe femtosecond transient ionization spectroscopy. DMNA is electronically excited to its S_1 state using a femtosecond pump pulse at 271 nm and subsequently ionized by a probe pulse at 406.5 nm. A pump pulse at 271 nm is chosen because excitation of DMNA at this wavelength is not of sufficient energy to dissociate the molecule on its S_1 PES through an NO₂ elimination pathway. Relaxation dynamics of DMNA from the S_1 excited state is probed as a function of time delay between the two femtosecond pulses. A very short lifetime of the DMNA S_1 state ($\sim 50 \pm 16$ fs) is determined. Such a short excited state lifetime most likely excludes the possibility of relaxation through singlet–triplet adiabatic state crossing in the energy deactivation of a nitramine. CASMP2//CASSCF calculations establish the singlet–singlet crossing point $(S_1/S_0)_{CI}$ is responsible for this fast decay of DMNA from its S_1 excited electronic state. Following its IC from S_1 to S_0 through the $(S_1/S_0)_{CI}$ CI, DMNA can either generate an NO₂ product through an N–N bond fission mechanism as a major channel, or generate an NO product through a nitro-nitrite isomerization mechanism as a minor channel. Details about the dissociation of DMNA on its S_0 surface could be found in ref 15b.

II. EXPERIMENTAL PROCEDURES

Detailed experimental procedures for femtosecond laser pump–probe spectroscopy have been described in our previous publications.^{15d,26} Briefly, the experimental setup consists of a femtosecond laser system, a supersonic jet expansion nozzle, and a time-of-flight mass spectrometer (TOFMS). For femtosecond pump–probe experiments, a 271 nm beam is used as the pump pulse,

and a second beam centered at 406.5 nm is used as the probe pulse. At zero time delay between the pump and probe pulse, only the DMNA parent ion is observed. By delaying the probe beam with respect to the pump beam, the S_1 excited state lifetime related to 271 nm excitation can be extracted from the pump–probe transient spectrum (TOFM spectral intensity vs pump–probe time delay) employing a single exponential decay function to fit the data.

The femtosecond laser light is generated by a femtosecond laser system consisting of a self-mode-locked Ti:Sapphire oscillator (KM Laboratories), and a homemade ring cavity Ti:Sapphire amplifier. The 406.5 and 271 nm laser beams, which are generated by two separate nonlinear β -BaB₂O₄ (BBO) crystals, are the second and third harmonics of the fundamental 813 nm femtosecond laser pulse. The energies of the 406.5 and 271 nm laser pulses are about 15 and 2 μ J, respectively. The cross-correlation of the two beams is measured via two-photon nonresonance ionization of the benzene molecule, which yields a time duration of the laser pulse of about 170 ± 8 fs.^{26c}

The experiment is run at a repetition rate of 10 Hz. The timing sequence for the pulsed nozzle, excitation laser, and ionization laser (both ns and fs) is controlled by a time delay generator (SRS DG535). The pulsed molecular beam is perpendicularly crossed by a UV laser in the excitation region of TOFMS. A background pressure of 1×10^{-5} Torr is maintained in the vacuum chamber during the experiment. Ion signals are detected by a microchannel plate detector (MCP). Signals are recorded and processed on a personal computer using a boxcar averager (SRS SR 250) and an analog-to-digital conversion (ADC) card (Analog Devices RTI-800). For femtosecond time-resolved experiments, the delay time between the pump and probe beam is controlled by a microtranslation stage (Thorlabs: LNR50SEK1) with a step size of 13 fs. Each point on the pump–probe transient spectrum corresponds to an average intensity resulting from 100 laser shots.

III. THEORETICAL PROCEDURES

All geometry optimizations relevant to excited electronic state decomposition of DMNA are executed at the CASSCF(14,11)/6-31G(d) level of theory employing the Gaussian 03 program.²⁷ No symmetry restrictions are applied to the calculations. To explore the excited state PESs of DMNA, an active space comprising 14 electrons distributed in 11 orbitals, denoted as CASSCF(14,11), is employed. A large active space, (14, 11), is employed for these CASSCF calculations, not necessarily to include dynamic correlation energy, which has been included in CASMP2 calculations, but for the CI calculations. Here CASMP2 calculation is not performed because energies calculated at the CASSCF level of theory show good agreement with the gas phase absorption maximum of DMNA, which indicates that the dynamic correlation is not important for the present system. Orbitals used in the active space are one N nonbonding $2S_N$ orbital, two NO bonding orbitals σ_{NO} , two NO antibonding orbitals σ_{NO}^{**} , one delocalized ONO π -bonding orbital π_{ONO} , one delocalized ONO π -antibonding orbital π_{ONO}^* , one bonding NN orbital σ_{NN} , one NN antibonding σ_{NN}^* , one π -nonbonding orbital $n\pi_O$, and one σ nonbonding $n\sigma_O$.^{15b} Vertical excitation energies are calculated by state averaging over the ground and various excited states with equal weight for each state. Critical point structures (minima and transition states) are characterized by analytical frequency calculations, and minimum energy paths are calculated using an intrinsic reaction coordinate

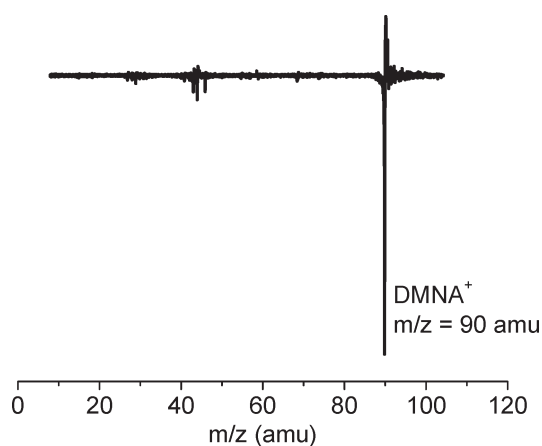


Figure 2. TOFMS of DMNA obtained at zero time delay between pump and probe pulses.

(IRC) algorithm implemented in the Gaussian 03 program.²⁷ As the present Gaussian code cannot perform analytical frequency calculations using more than eight orbitals in the active space, frequency calculations and IRC calculations, which require initial force constants, are performed using a reduced active space (10,7) (σ_{NO} and σ_{NO^*} bonding and antibonding are omitted) with the same basis set.²⁷

IV. EXPERIMENTAL RESULTS

Figure 2 shows the TOFMS obtained through photoionization of DMNA at zero time delay between the ~ 170 fs pump and probe pulses. Only the parent ion is observed; no fragment ion signals are observed at zero time delay between pump and probe pulses. To probe relaxation dynamics of DMNA from the S_1 electronically excited state generated at 271 nm, a fs pump–probe experiment is performed. In this experiment, a pump pulse (one photon) at 271 nm is used to excite the parent molecule to the S_1 state, and a probe pulse (two photons) at 406.5 nm is used to ionize the molecule from the S_1 state. Pump beam fluence is reduced such that two photon ionization of DMNA by the single pump beam is avoided. The fs probe pulse at 406.5 nm can only ionize DMNA if the S_1 state remains populated following the fs pump pulse. Therefore, as the time delay between pump and probe pulses is increased, a change in the parent ion signal intensity in TOFMS is observed. If the ion intensity is monitored as a function of pump and probe delay time, a transient ionization spectrum is recorded which contains dynamical information on the depopulation of the S_1 state. Deconvolution of the transient ionization spectrum from cross correlation of the pump and probe pulses provides a single exponential decay with a decay constant that corresponds to the lifetime of the S_1 excited state of DMNA.

The above considerations are evident in Figure 3, which displays the pump–probe transient ionization spectrum obtained by monitoring the DMNA parent ion signal at $m/z = 90$ amu as a function of pump–probe delay time. Deconvolution of the pump–probe transient spectrum from pump–probe pulse cross correlation gives a single exponential decay with a decay constant of $\sim 50 \pm 16$ fs. Since the signal exponential decay is induced due to the depletion of the excited S_1 state population of DMNA, we interpret the decay time constant to be the lifetime of the S_1 state of DMNA. To the best of our knowledge, this is the first time that the lifetime of the excited S_1 state of DMNA is determined. The

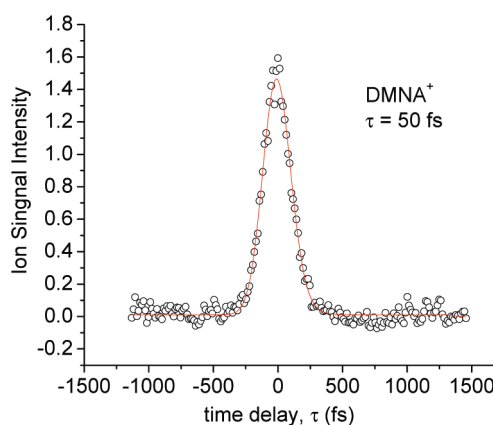


Figure 3. Femtosecond pump–probe transient spectrum for the DMNA parent following its electronic excitation at 271 nm. A 406.5 nm laser pulse is used as the probe beam. Open circles are experimental measurements; the solid line is a fit with a Gaussian cross correlation spectrum and a single exponential decay. The transient spectrum shows a fast exponential decay (50 ± 16 fs) of the $S_1(n,\pi^*)$ excited electronic state of DMNA.

ultrafast lifetime of the S_1 state can well explain the broad absorption spectrum around the $S_1 \leftarrow S_0$ transition of DMNA.²⁸ Radiative emission from this state would be quenched by this fast IC event. Further details of this IC pathway are given in the Theoretical Results section.

V. THEORETICAL RESULTS

The CASSCF(14,11)/6-31G(d) calculated vertical excitation energies for the two lowest lying excited electronic states (S_1 and S_2) of DMNA are 5.13 and 5.5 eV, respectively. The S_1 and S_2 states are of (n,π^*) character. The calculated vertical excitation energy (5.5 eV) of the S_2 state is in good agreement with the available experimental absorption maximum value of 5.31 eV.²⁸ Direct comparison of the excitation energy (4.57 eV at 271 nm) used in the present experimental work with the calculated vertical excitation energies (5.13 and 5.5 eV for S_1 and S_2 states, respectively) reveals that DMNA is excited below the Franck-Condon (FC) point of the S_1 state by electronic excitation of the molecule at 271 nm.

In order to determine the relaxation path involved in fast IC of DMNA from the S_1 state, the minimum energy, steepest decent path connecting the FC points of S_1 and S_0 surfaces of DMNA to the minimum energy $(S_1/S_0)_{\text{CI}}$ CI is determined (see Figure 4). This path is computed at the CASSCF(14,11)/6-31G(d) level of theory. The reaction pathways from the FC point on S_1 to the S_1/S_0 CI, and from the S_1/S_0 CI back to the ground state minimum are different in Figure 4, and the plot is sketched for energy with respect to number of steps, which is computed through the IRC algorithm based on the phase that is associated with the bending mode of the N–NO₂ moiety. Figure 4 shows that vertical excitation of DMNA to even below the FC point of the S_1 PES can potentially lead to a nonadiabatic IC of electronically excited DMNA from the S_1 PES to the S_0 PES through the $(S_1/S_0)_{\text{CI}}$ CI. This CI is energetically accessible even below the FC point of the S_1 PES because no energy barrier exists in this reaction pathway. Molecular structure of DMNA at $(S_1/S_0)_{\text{CI}}$ shows a bent N–NO₂ moiety.

The N–NO₂ bond dissociation reaction paths on the S_1 and S_0 PESs of DMNA can also be investigated by elongating the N–NO₂ bond length, as plotted in Figure 5. Note that the

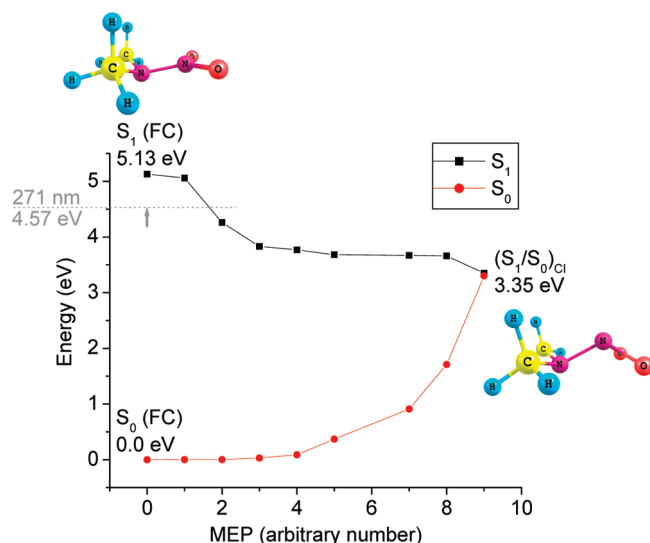


Figure 4. Minimum energy pathways from the FC point to the $(S_1/S_0)_{CI}$ CI following S_1 and S_0 energy gradients for DMNA, computed using the IRC algorithm at the CASSCF(10,7)/6-31G(d) level of theory. The energies are recalculated at the CASSCF(14,11) theory level.

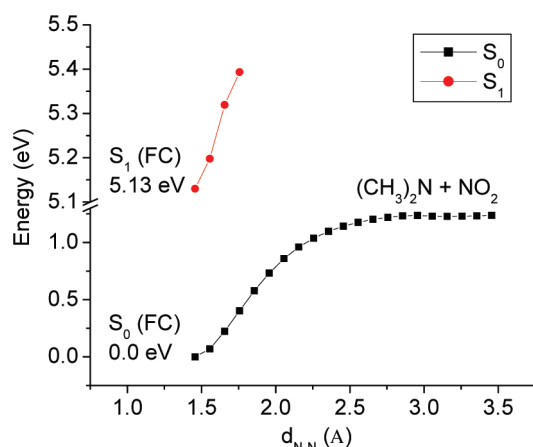


Figure 5. N–NO₂ bond dissociation pathways for DMNA on the S_0 and S_1 PESs, computed using the potential energy scan algorithm at the CASSCF(14,11)/6-31G(d) level of theory. All geometrical parameters, except the N–NO₂ bond distance, were optimized during the scan.

reaction coordinate for the curves represented in Figure 5 is different from that presented in Figure 4. An N–NO₂ bond dissociation barrier of more than 10 kcal/mol is predicted for DMNA with respect to the FC point on the S_1 surface for this coordinate. Since electronic excitation at 271 nm excites DMNA below its FC point on the S_1 PES, the adiabatic N–NO₂ bond dissociation pathway on the S_1 surface is not accessible, because it requires more than 10 kcal/mol activation energy from the FC point of the S_1 surface.

Thus, theoretical calculations yield that electronic excitation of DMNA at 271 nm populates the S_1 excited electronic state PES upon which DMNA is not able to undergo adiabatic N–NO₂ bond dissociation. The isomerization channel, which has been discussed in detail in our previous publication,^{15b} can be important if we excite the molecule to the S_2 state. Other decomposition routes, such as C–H bond dissociation, are much higher in energy and not accessible to the molecule from the S_1 state PES.

Instead, following electronic excitation at 271 nm, DMNA can undergo IC to the ground electronic state PES. This non-adiabatic radiationless transition occurs through the $(S_1/S_0)_{CI}$ CI.

IV. DISCUSSION

An ultrafast lifetime of $\tau \sim 50 \pm 16$ fs is determined for the $S_1(n,\pi^*)$ excited electronic state of DMNA following its electronic excitation at 271 nm, using femtosecond pump–probe spectroscopy. Theoretical calculations at the CASSCF(14,11)/6-31G(d) theory level show that the $(S_1/S_0)_{CI}$ CI in the relaxation pathway involving IC of DMNA from its S_1 PES to its S_0 PES is responsible for the ultrashort lifetime of the $S_1(n,\pi^*)$ excited electronic state. A PES scan along the N–NO₂ bond dissociation pathway computed at the same level of theory indicates that DMNA does not have sufficient energy to surmount the adiabatic N–NO₂ bond dissociation barrier on the S_1 PES following its electronic excitation at 271 nm; hence, only the nonadiabatic relaxation pathway through the $(S_1/S_0)_{CI}$ is open for DMNA following excitation at 271 nm. Geometry near the CI shows that an out of plane NO₂ bending mode with respect to the N–NO₂ plane is involved in this relaxation/dissociation pathway, which is barrierless on the S_0 surface.

DMNA is considered to be a model system for nitramine energetic materials: this molecule is expected to evidence electronic properties of large and more complex nitramine energetic materials. Following electronic excitation of DMNA at 271 nm, the molecule can rapidly come back to the ground state, transferring electronic excitation energy to its vibrational degrees of freedom. An ultrafast lifetime of the lowest lying S_1 excited state of DMNA corroborates the fact that nitramine molecules are able to convert their initial electronic excitation energy to vibrational energy on their ground state PES. This behavior could be general for all nitramine systems, including large and complex energetic materials such as RDX; however, corroboration of such a consideration for true energetic systems requires further study of excited electronic states of large energetic systems.

The full mechanism for molecular explosive behavior and sensitivity is still not completely revealed. Thus far, many factors, such as chemical stability, structure, crystal density, etc. have been suggested to play a present role in the coherent description of nitramine molecular explosive behavior. In this work, we demonstrate that the ultrashort lifetime of the excited electronic state of nitramine molecules can be an important factor controlling their explosive behavior.

VII. CONCLUSION

Utilizing synergism between experiment and theory, the $S_1 \rightarrow S_0$ IC dynamics of a model nitramine energetic molecule, DMNA, is determined. Electronic excitation of DMNA to the S_1 state promotes an electron from an $n\sigma_O$ to a π^* orbital, which initially localizes the electronic excitation energy on the NO₂ moiety and activates a bending mode of the NO₂ moiety with respect to the N–NO₂ plane. This bending mode is responsible for an ultrafast ($\sim 50 \pm 16$ fs) IC of DMNA from its S_1 excited state to its S_0 ground electronic state. This fast relaxation quenches radiative processes from the S_1 surface of DMNA. The present study reveals the nature of the electronic energy distribution generated in the $S_1 \rightarrow S_0$ electronic transition and the mechanism of energy transfer to the S_0 vibrational motion. This new insight into nitramine energy dynamics should lead to a much deeper understanding of

molecular explosive behavior of nitramine energetic materials, in general.

AUTHOR INFORMATION

Corresponding Author

*E-mail: erb@lamar.colostate.edu.

Present Addresses

[†]Chemistry Department, Brookhaven National Laboratory, Upton, NY 11961, USA.

REFERENCES

- (1) Bernstein, E. R. *Overviews of Recent Research on Energetic Materials*; Thompson, D., Brill, T., Shaw, R., Eds.; World Scientific: Hackensack, NJ, 2004.
- (2) Williams, F. E. *Adv. Chem. Phys.* **1971**, *21*, 289.
- (3) Sharma, J.; Beard, B. C.; Chaykovsky, M. J. *Phys. Chem.* **1991**, *95*, 1209.
- (4) Gilman, J. J. *Philos. Mag. B* **1995**, *71*, 1057.
- (5) Kuklja, M. M.; Aduv, B. P.; Aluker, E. D.; Krashenin, V. I.; Krechetov, A. G.; Mitrofanov, A. Y. *J. Appl. Phys.* **2001**, *89*, 4156.
- (6) Windawi, H. M.; Varma, S. P.; Cooper, C. B.; Williams, F. J. *Appl. Phys.* **1976**, *47*, 3418.
- (7) Schanda, J.; Baron, B.; Williams, F. *Acta Techn. Acad. Sci. Hungaricae* **1975**, *80*, 185.
- (8) Schanda, J.; Baron, B.; Williams, F. J. *Lumin.* **1974**, *9*, 338.
- (9) Varma, S. P.; Williams, F. J. *Chem. Phys.* **1973**, *59*, 912.
- (10) Hall, R. B.; Williams, F. J. *Chem. Phys.* **1973**, *58*, 1036.
- (11) Williams, F. *Adv. Chem. Phys.* **1971**, *21*, 289.
- (12) Dremin, A. N.; Klimenko, V. Y.; Davidova, O. N.; Zoludeva, T. A. Proceedings of the 9th Symposium on Detonation, Portland OR, 1989; (Office of Naval Research, Arlington); p725.
- (13) Sharma, J.; Forbes, J. W.; Coffey, C. S.; Liddiard, T. P. *J. Phys. Chem.* **1987**, *91*, 5139.
- (14) Sharma, J. *APS Topical Meeting on Shocks in Energetic Materials*, Williamsburg VA, 1991.
- (15) (a) Bhattacharya, A.; Guo, Y. Q.; Bernstein, E. R. *Acc. Chem. Res.* **2011**, *43*, 1476. (b) Bhattacharya, A.; Guo, Y. Q.; Bernstein, E. R. *J. Phys. Chem. A* **2009**, *113*, 811. (c) Bhattacharya, A.; Guo, Y. Q.; Bernstein, E. R. *J. Chem. Phys.* **2009**, *131*, 194304. (d) Guo, Y. Q.; Bhattacharya, A.; Bernstein, E. R. *J. Chem. Phys.* **2008**, *128*, 034303.
- (16) Domcke, W.; Yarkony, D. R.; Koppel, H. *Conical Intersections: Electronic Structure, Dynamics and Spectroscopy*; World Scientific: Hackensack, NJ, 2003.
- (17) Worth, G. A.; Cederbaum, L. S. *Annu. Rev. Phys. Chem.* **2004**, *55*, 127.
- (18) Baer, M.; Billing, G. D. *The Role of Degenerate States in Chemistry*; Prigogine, I., Rice, S. A., Eds.; Advances in Chemical Physics; John Wiley & Sons: New York, 2002; Vol. 124.
- (19) von Neumann, J.; Wigner, E. Z. *Phys.* **1929**, *30*, 467.
- (20) Soto, J.; Arenas, J. F.; Otero, J. C.; Pelaez, D. *J. Phys. Chem. A* **2006**, *110*, 8221.
- (21) Serrano-Andres, L.; Merchan, M.; Borin, A. C. *Proc. Natl. Acad. Sci. U.S.A.* **2006**, *103*, 8691.
- (22) Ismail, N.; Blancafort, L.; Olivucci, M.; Kohler, B.; Robb, M. A. *J. Am. Chem. Soc.* **2002**, *124*, 6818.
- (23) Blancafort, L. *J. Am. Chem. Soc.* **2006**, *128*, 210.
- (24) Canuel, C.; Elhanine, M.; Mons, M.; Piuze, F.; Tardivel, B.; Dimicoli, I. *Phys. Chem. Chem. Phys.* **2006**, *8*, 3978.
- (25) Manaa, M. R.; Fried, L. E. *J. Phys. Chem. A* **1999**, *103*, 9349.
- (26) (a) Greenfield, M.; Guo, Y. Q.; Bernstein, E. R. *Chem. Phys. Lett.* **2006**, *430*, 277. (b) Guo, Y. Q.; Greenfield, M.; Bhattacharya, A.; Bernstein, E. R. *J. Chem. Phys.* **2007**, *127*, 15430. (c) Guo, Y. Q.; Bhattacharya, A.; Bernstein, E. R. *J. Phys. Chem. A* **2009**, *113*, 85.
- (27) Frisch, M. J.; Trucks, G. W.; Schlegel, H. B.; Scuseria, G. E.; Robb, M. A.; Cheeseman, J. R.; Montgomery, Jr., J. A.; Vreven, T.; Kudin, K. N.; Barone, V.; Mennucci, B.; Cossi, M.; Scalmani, G.; Rega, N.; Petersson, G. A.; Nakatsuji, H.; Hada, M.; Ehara, M.; Toyota, K.; Fukuda, R.; Hasegawa, J.; Ishida, M.; Nakajima, T.; Honda, Y.; Kitao, O.; Nakai, H.; Klene, M.; Li, X.; Knox, J. E.; Hratchian, H. P.; Cross, J. B.; Bakken, V.; Adamo, C.; Jaramillo, J.; Gomperts, R.; Stratmann, R. E.; Yazyev, O.; Austin, A. J.; Cammi, R.; Pomelli, C.; Ochterski, J. W.; Ayala, P. Y.; Morokuma, K.; Voth, G. A.; Salvador, P.; Dannenberg, J. J.; Zakrzewski, V. G.; Dapprich, S.; Daniels, A. D.; Strain, M. C.; Farkas, O.; Malick, D. K.; Rabuck, A. D.; Raghavachari, K.; Foresman, J. B.; Ortiz, J. V.; Cui, Q.; Baboul, A. G.; Clifford, S.; Cioslowski, J.; Stefanov, B. B.; Liu, G.; Liashenko, A.; Piskorz, P.; Komaromi, I.; Martin, R. L.; Fox, D. J.; Keith, T.; Al-Laham, M. A.; Peng, C. Y.; Nanayakkara, A.; Challacombe, M.; Gill, P. M. W.; Johnson, B.; Chen, W.; Wong, M. W.; Gonzalez, C.; Pople, J. A. *Gaussian 03*, revision C.02, Gaussian, Inc.: Wallingford CT, 2004.
- (28) McQuaid, M. J.; Sausa, R. C. *Appl. Spectrosc.* **1991**, *45*, 916.